Electronic structure and optical properties of Am monopnictides

D. B. Ghosh and S. K. De
Department of Materials Science, Indian Association for the Cultivation of Science, Jadavpur, Calcutta 700 032, India

P. M. Oppeneer
Department of Physics, Uppsala University, Box 530, S-751 21 Uppsala, Sweden

M. S. S. Brooks*
European Commission, Joint Research Centre, Institute for Transuranium Elements, Postfach 2340, D-76125 Karlsruhe, Germany
(Received 31 January 2005; revised manuscript received 7 June 2005; published 28 September 2005)

The ground-state and optical properties of the americium monopnictides, AmX (X=N, P, As, Sb, and Bi) are investigated theoretically on the basis of first-principles electronic structure calculations, employing the local density approximation (LDA) as well as the LDA+U approach. The LDA predicts pseudogap-like behavior in AmN and narrow gap (39–78 meV) semiconducting behavior in AmP to AmBi at ambient conditions. The LDA+U calculations predict semiconducting behavior with a real gap of 192 meV for AmN and a pseudogap in AmP to AmBi. The computed semiconducting or pseudogap character is in fine agreement with the first photoemission experiments performed on AmN and AmSb films by Gouder *et al.* [preceding paper, Phys. Rev. B **72**, 115122 (2005)]. This property is shown to result from the strong Am spin-orbit interaction, the Coulomb repulsion, and the particular *p-d-f* hybridizations. The calculated equilibrium lattice constants obtained for the AmX series using the LDA+U technique are in good agreement with available experimental data. Also, the binding energies of the 5*f*s computed with the LDA+U approach correspond well to 5*f* binding energies deduced from the photoemission spectra measured by Gouder *et al.* The high, temperature-independent paramagnetic susceptibilities of the AmX are successfully explained by a Van Vleck mechanism. A pressure-induced valence transition at high pressure is predicted for AmN.

DOI: 10.1103/PhysRevB.72.115123 PACS number(s): 71.28.+d., 71.20.−b, 78.20.−e

I. INTRODUCTION

The lanthanide (4*f*) and actinide (5*f*) elements and their compounds exhibit a rich variety of electronic and magnetic properties. The complex behavior of the *f* electrons in both series play a crucial role in their intriguing physical properties. As one among the various extraordinary properties, *f*-electron systems may exhibit a gap in the electronic spectrum. Such behavior has been intensely investigated in the case of 4*f* materials, where some of the interesting materials are categorized, for example, as wide-gap magnetic semiconductors or narrow-gap (~5–50 meV) mixed-valence and heavy-fermion semiconductors.[2–4] For 4*f* systems, the latter type of semiconductors occurs frequently and they are often referred to as Kondo insulators,[5] where the gap formation is generally attributed to a correlated magnetic coupling of valence electrons to the isolated local magnetic moments of *f* electrons. The understanding of the origin of the small gap is still a complicated issue in the field of strongly correlated *f*-electron systems. The behavior of 5*f* electrons is distinct from that of the 4*f*s, because a sizable hybridization between the *f* and other band states is possible, as has been shown in various experimental and theoretical investigations.[6–9] However, correlated electron behavior and gap formation do occur as well,[10–12] which, with regard to the hybridization-induced broadening of the *f* states, require additional theoretical considerations. To understand the possible reasons for narrow-gap formation in 5*f*-electron systems, more studies exploring such systems are required.

One important aspect of interest in 5*f*-electron systems is the degree of localization of the *f* states. Within the series of the actinide elements, the transition from delocalized 5*f* states to localized 5*f* states occurs at around Pu.[13,14] Americium, the element to the right of Pu in the Periodic Table, shows anomalous behavior in its lattice constant. The sudden jump in the lattice constant along the actinide series of about 10% is attributed to the localization of the 5*f* states and their withdrawal from the bonding. The photoemission spectrum[1,15] indicates that the 5*f* states of Am are localized and are located some 1–3 eV below the Fermi level. However, the degree of localization depends on the atomic distances as well as on the chemical environment, which may induce level broadening due to hybridization effects. For example, for Am metal under pressure, discontinuous changes in the lattice constant have been recently observed, which were ascribed to a delocalization of the 5*f*s.[16] Hence, the behavior of the 5*f* electrons in Pu or Am compounds may vary, on account of the atomic distances and the 5*f* ligand or 5*f*-6*d* hybridization. For example, 5*f*-derived states were observed in the vicinity of the Fermi level in the Pu monochalcogenides and in the superconductor $PuCoGa_5$, in spite of the larger Pu—Pu separation.[17–19] The equilibrium lattice constants of the actinide monopnictides[20,21] demonstrate that the Am pnictides do not follow the monotonic contracting trend with the atomic number that is typical for the lanthanide pnictides. In the same manner as the behavior of the lattice parameters of the early actinides reflects delocalized, bonding 5*f* states,[13] this is an indication that the 5*f*s in the Am monopnictides are still delocalized to some extent. The

TABLE I. Comparison of experimental (Refs. 20 and 36) and calculated equilibrium lattice parameters of the americium monopnictides. Given are the experimental lattice constant (a_{expt}), the LDA result (a_{LDA}), and the LDA+U result for U=2.5 eV (in Å). For the LDA+U calculation, the corresponding bulk moduli B_0 in GPa and the pressure derivative of the bulk modulus B_0' are also given.

			LDA+U (U=2.5 eV)		
	a_{expt}	a_{LDA}	a	B_0	B_0'
AmN	4.995	4.606	4.825	189.37	4.509
AmP	5.711	5.219	5.432	115.77	3.806
AmAs	5.876	5.400	5.592	102.27	4.401
AmSb	6.240	5.854	6.003	89.48	3.851
AmBi	6.338	5.991	6.076	77.80	4.527

actinide (U, Np, Pu) monopnictides reveal highly anisotropic ferromagnetic and antiferromagnetic spin structures at low temperatures.[22] In contrast, for the americium monopnictides, experimental magnetization studies suggest temperature-independent paramagnetism corresponding to a trivalent Am ion (i.e., $5f^6$, J=0 state).[23–25] A similar paramagnetic behavior was observed also for the Pu monochalcogenides.[26] On account of the combination of nonmagnetic and narrow-gap semiconducting behavior, the Pu monochalcogenides have been argued to be intermediate valence materials, i.e., a $5f$ analogue of SmS in the $4f$ series.[27] Thus, the Am monopnictides, which are isoelectronic to the Pu monochalcogenides are attractive systems in which unusual electronic phenomena may appear in conjunction with the dual character (bandlike vs localized) of the $5f$ electrons. Indeed, the experimental photoelectron spectroscopy study,[1] conducted in conjunction with the present theoretical investigation, reveals intriguing semiconducting or pseudogap behavior of the Am monopnictides.

The ground-state properties of the light actinides are quite well described by the local spin-density approximation (LSDA) (e.g., see Ref. 28). The LSDA description of the $5f$ electrons has been used for the U monochalcogenides and monopnictides.[29,30] Oppeneer *et al.*[21] have carried out a detailed study of the electronic, optical, and magnetic properties of Pu monochalcogenides employing the LSDA. They obtained pseudogap behavior due to the combination of $5f$ hybridization and spin-orbit (SO) splitting of $5f$ states, which is consistent with the semiconducting behavior observed in transport studies.[10] Electronic structure calculations for various actinide rocksalt compounds, including the Am monopnictides were recently performed by Petit *et al.*,[31] who employed the self-interaction correction to the local spin-density approximation (SIC-LSDA). In the SIC-LSDA approach, the number of $5f$ electrons that are treated as localized can be chosen. Considering various possible valences, Petit *et al.* computed the trivalent Am configuration to be the most favorable one for all Am monopnictides.

In spite of the isoelectronic configuration ($5f^6$) of divalent Pu in monochalcogenides and trivalent Am in monopnictides and the identical magnetic behavior, the stronger tendency to localized behavior of the $5f$ electrons in Am suggests that incorporating correlation effects in the LDA is essential for the treatment of compounds containing transplutonium elements. This stimulated us to investigate thoroughly the electronic and optical properties of the Am monopnictides using both the LDA and LDA+U approaches. The LDA+U scheme has recently been successfully used to describe the electronic properties of $4f$ and $3d$ systems. For actinide systems, the LDA+U approach has been used for some uranium compounds,[32] only recently, it has been applied to transuranium materials,[33–35] but not yet to transplutonium materials. The main aim of the present work is to obtain an electronic structure picture that is consistent with the available physical properties for the Am monopnictides.

II. COMPUTATIONAL DETAILS

The americium monopnictides AmX (X=N, P, As, Sb, and Bi) crystallize in the rocksalt structure at ambient conditions. The experimental lattice parameters[20,36] of the Am monopnictides are listed in Table I. We carried out relativistic, full-potential (FP) self-consistent band-structure calculations, using the linear muffin-tin orbital (LMTO) method[37] in the FP-LMTO version as developed by Savrasov *et al.*[38] The atomiclike basis consists of $7s, 6p, 6d, 5f$ orbitals for Am and of $(n)s$, $(n)p$, and $(n)d$ for the pnictogen atom, where n refers to the principal quantum number. The $6s$ electrons of Am and $(n-1)d$ electrons of As and Sb were treated in a separate panel and, hence, were not included in the optical calculations to be presented below. The core states were treated fully relativistically, while for the valence states spin-orbit coupling was included using a second variational procedure. In the self-consistent calculations, we used 242 k points in the irreducible Brillouin zone (BZ). The same number of k points was used for the evaluation of the optical momentum matrix elements.

The electronic structure has been calculated by the standard LDA method in which the $5f$ electrons are treated as delocalized. The exchange-correlation potential in the LDA was calculated using the Vosko-Wilk-Nussair parametrization. In the LDA+U approach, the density-functional formalism is modified in order to include the strong correlations among the f electrons. In the atomic-limit LDA+U method,[39] the LDA energy functional is modified by removing the LDA f-f interactions and replacing these by the on-site Coulomb interaction among the f electrons. Theoretical

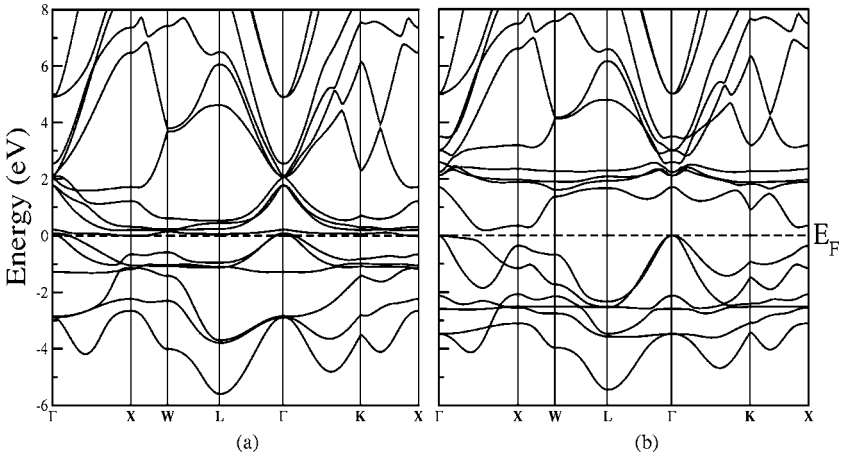

FIG. 1. Energy-band structure of AmN, computed with (a) the LDA approach and (b) the LDA+U (U=2.5 eV) approach at the experimental lattice constant.

details of the calculation were given in a previous paper.[40]

The calculations were performed for different U values, which will be discussed in detail below. The other required Slater integrals F^2, F^4, and F^6 for f electrons have been adopted from the paper by Ogasawara *et al.*[41] to calculate the matrices $U_{mm'}$ and $J_{mm'}$. The paramagnetic calculations have been performed by placing three of the six f electrons in the spin-up direction with orbital-momentum quantum number, $m_l=-3,-2,-1$, and the other three in the spin-down direction with $m_l=+3,+2,+1$,[42] i.e., the $j_{5/2}$ states are effectively shifted downward by the Coulomb U while the $j_{7/2}$ states are shifted upward.[43]

III. ELECTRONIC STRUCTURES

A. Energy-band structures

To start with, the energy-band structures of the AmX compounds have been calculated for the experimental lattice constants using the LDA. Within the LDA, we calculate all Am monopnictides—except AmN—to be narrow-gap semiconductors, see Figs. 1 and 2. AmN differs in its electronic structure from the other pnictides mainly because of its smaller lattice parameter (see Table I). Correspondingly, the larger f overlap gives rise to a larger f bandwidth; therefore, the 5f bands near the Fermi energy (E_F) become somewhat more dispersive and, thereby, straddle the Fermi level, thus, closing the gap. The small gap values obtained for Am phosphide to bismuthide are listed in Table II. There exist both direct and indirect gaps. The latter correspond to the maximum of the valence band at the Γ point and minimum of the conduction band at the X or the L point, respectively. The size of the indirect energy-band gaps is calculated to vary from 39 to 78 meV (see Table II), whereas the direct, optical-band gaps are larger, of the order of 150 meV. The basic origin of the gap formation is the strong Am spin-orbit interaction, which splits away the $5f_{5/2}$ and $5f_{7/2}$ subbands to below and above E_F, respectively.[44] As shown before for the Pu monochalcogenides, here also the particular hybridization of the 5fs plays a role in the gap formation.[21] As our calculations are based on density-functional theory, it could be that the computed gaps underestimate the actual, experimental ones.[45]

Next, we calculated the energy-band structures of the Am monopnictides using the LDA+U approximation, in which the U can suitably be chosen within a range of values (~1–4 eV), which are in the ballpark of commonly accepted values for actinides.[46] The calculated energy bands of AmN using the LDA+U, with U=2.5 eV, is shown in Fig. 1 as well. As can be expected, the Coulomb repulsion drastically modifies the energy positions of the f states. The inclusion of the U shifts the occupied $f_{5/2}$ subband further downward and the unoccupied $f_{7/2}$ subband further upward from the Fermi level. This leads to differences in the energy bands near E_F

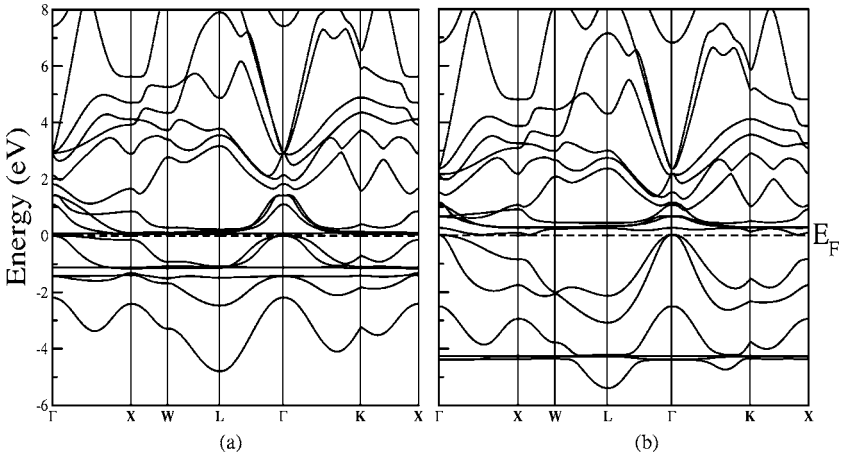

FIG. 2. As with Fig. 1, but for AmBi.

TABLE II. The energy gaps E_g of the Am monopnictides as computed using the LDA and LDA+U (U=2.5 eV) approaches. The LDA+U values given are the indirect gap for AmN and direct gaps for the other Am monopnictides. The LDA gap values given are the indirect gaps. Also listed are the experimental temperature-independent susceptibilities χ_{expt}.

	E_g^{LDA} (meV)	E_g^{LDA+U} (meV)	χ_{expt} (10^{-6} emu/mol)
AmN	pseudogap	192	777
AmP	59	266	—
AmAs	65	256	550
AmSb	78	228	1250
AmBi	39	224	—

as compared to the LDA calculation. For example, the LDA+U produces a real gap of 192 meV in AmN (see Table II). For the other Am monopnictides, the LDA+U approach yields a pseudogap at E_F. The energy bands of AmBi calculated for the same U value are shown in Fig. 2. The occupied $f_{5/2}$ states appear now at the bottom of the p states of Bi and are almost dispersionless except around the L point and along the Γ-K direction. For all Am monopnictides, except AmN, the top of the pnictogen p-derived valence band just touches the Fermi level at the Γ point, whereas an unoccupied band bends down and touches the Fermi level near the X point (cf. Fig. 2). The indirect gap vanishes and consequently the LDA+U predicts for U=2.5 eV only pseudogap behavior for the AmX (X=P, As, Sb, and Bi). In these monopnictides there exists, however, a direct, optical gap between the two aforementioned bands, which is of the order of 200–300 meV (see Table II). Furthermore, we mention that for a smaller U value of 1 eV, the LDA+U energy bands are still relatively close to those of the LDA calculation and a real band gap is obtained for all AmX compounds.

The photoelectron experiments[1] performed on AmN and AmSb films confirm the insulating or pseudogap character of these two Am pnictides. For AmN, the photoemission intensity measured with He I and He II radiation smoothly vanishes at the Fermi level. For AmSb, the intensities at E_F become very small, but are not completely zero. Thus, AmN is likely a semiconductor, whereas AmSb could exhibit a pseudogap. However, it cannot completely be excluded that some inhomogeneity in the AmSb films is responsible for the residual intensity.[1]

B. Densities of states

The angular momentum decomposed LDA+U density of states (DOS) of the AmX compounds are shown in Fig. 3 for U=2.5 eV. The DOS of all the pnictides are very similar as can be expected. The two huge peaks below and above the Fermi level are derived from the SO-split f states of Am. For all Am pnictides the six Am $f_{5/2}$ bands are fully occupied and located in the region of significant pnictogen p partial DOS. A sizable contribution from the Am d states can also be observed in the same region. The eight Am $f_{7/2}$ bands are located above E_F. The similarity in the shapes of the partial

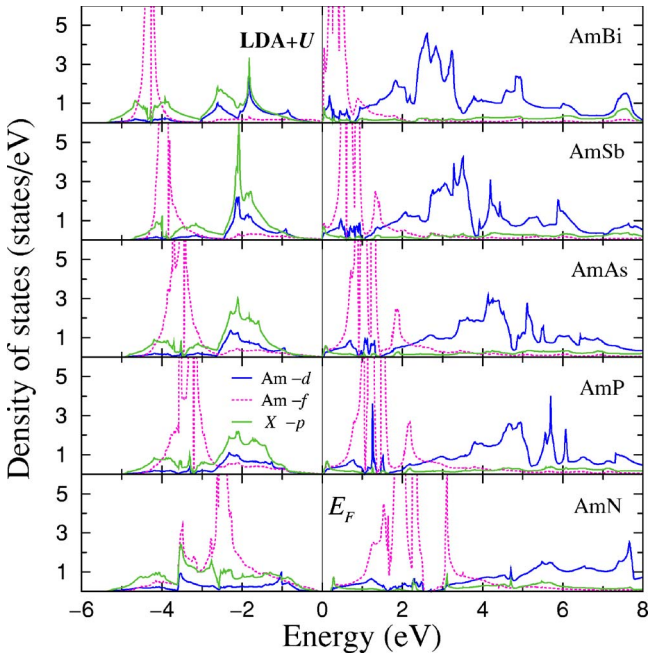

FIG. 3. (Color online) LDA+U partial densities of states of the Am monopnictides computed for U=2.5 eV.

DOS indicate significant p-d, d-f, and p-f hybridizations. The gap (for AmN) or pseudogap is formed within hybridized p-d-f bands. Some characteristic changes in the AmX series occur due to the increase of the lattice parameter and the SO interaction with the atomic number from N to Bi. The increased SO interaction leads to an increased splitting of the p bands, causing the top of the p bands to move closer to E_F. The lattice parameter increase (see Table I) reduces the f ligand overlap and the already small f-f overlap and, consequently, the 5f bandwidth. The occupied f levels shift away from E_F while the unoccupied f levels move closer to E_F. Also the hybridizations among the f and p, d states become less due to the narrowness and shift of the 5f band centers. Nevertheless, the hybridizations of the p-d-f states are, for the heavier pnictides, still sufficient to support the pseudogap formation.

The features shown in the LDA+U partial DOS (Fig. 3) correspond quite well to the photoemission spectra obtained with He I and He II radiation.[1] The He I-He II difference spectra reveal the approximated binding energy positions of the 5f states (He II-He I spectrum) as well as of the pnictogen p states (He I-He II spectrum). The Am-5f states occur at binding energies of 2.5 and 3.3 eV for AmN and AmSb, respectively (see Figs. 3 and 4 in Ref. 1). The LDA+U (U =2.5 eV) calculations give 5f binding energies of ~2.5 and 4 eV for AmN and AmSb, respectively. Although atomic multiplets might influence the photoemission spectra, the calculations do provide a similar shift toward higher binding energies for the heavier antimonide. The position of the pnictogen p band shows the opposite trend: the nitrogen p band occurs experimentally at ~3.8 eV, the antimonide p band at 2 eV. The LDA+U calculations place the main p partial DOS below 3 eV for AmN and at about 2 eV for AmSb. Furthermore, the photoelectron spectra reveal that the pnic-

togen p band decreases smoothly from its extremal energy position toward the Fermi energy. This occurs for the computed p partial DOS, too, which decreases toward, and vanishes at, E_F (see Fig. 3).

Within the Am monopnictide series, the calculated LDA $+U$ $5f$-occupation numbers vary from 5.97 to 6.10, for AmN to AmBi, respectively. The Am valency is thus close to trivalent, as one would expect. For smaller lattice constants, the f-occupation number diminishes and the d-occupation number accordingly increases. For AmN this suggests that possibly a valence transition from trivalent to tetravalent Am occurs under pressure, which would render mixed valency behavior in compressed AmN.

The properties of AmN are different from the other monopnictides on account of its small lattice constant. To study the effect of the lattice constant on the electronic structure, we calculated both the LDA and LDA$+U$ band structures of AmN as a function of the lattice parameter. Using the LDA, at the experimental lattice constant two (doubly degenerate) bands near the Γ point and one band near the X point just cross the Fermi level E_F and consequently give rise to metallic behavior. As the lattice parameter increases, the bands near the Γ point move slightly downward from E_F while the other band at X moves slightly upward, sufficient to open a gap at E_F. Noticeable changes do not occur at the other high-symmetry points and axes. Thus, for AmN, the LDA predicts the opening of a gap for a larger lattice constant in between 5.15 to 5.29 Å. Within the LDA$+U$, on the other hand, there already exists a gap which becomes reduced under pressure due to a *broadening* of the f bandwidth and reaches zero for pressures around 40 GPa. For AmN the width of the f band, thus, plays a role in the gap formation, in addition to the SO splitting.

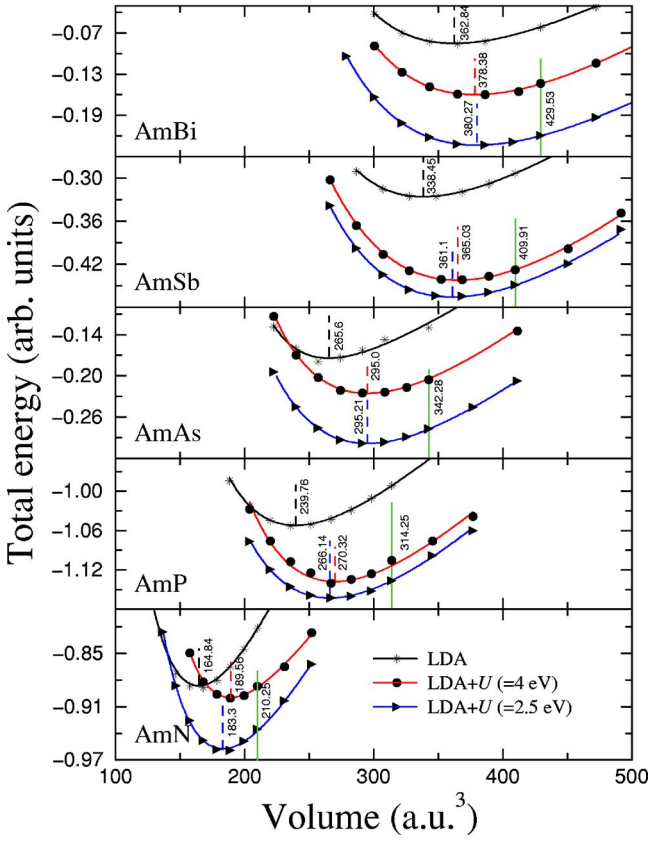

FIG. 4. (Color online) The total energy versus volume for the Am monopnictides as obtained from LDA and LDA$+U$ calculations (U=2.5 and 4 eV). The experimental equilibrium volumes are indicated by the straight green lines.

C. Calculated lattice parameters

The equilibrium lattice parameters of the AmX have been determined from total-energy calculations by the standard LDA as well as LDA$+U$ methods. The calculated total energies versus unit-cell volume along with the available experimental values[20,36] are shown in Fig. 4 for U=2.5 eV and 4 eV together with the LDA result. The most notable finding is that the equilibrium volumes given by the LDA$+U$ total-energy calculation are much closer to the experimental value than the corresponding LDA data. The equilibrium volume V_0 is determined here by fitting the total energy by Murnaghan's equation of state

$$E(V) - E_0 = \frac{B_0 V}{B_0'}\left[\frac{\left(\frac{V_0}{V}\right)^{B_0'}}{B_0' - 1} + 1\right], \qquad (1)$$

where E_0 is an arbitrary constant, B_0 is the bulk modulus, and B_0' its pressure derivative. The best-fitted equilibrium lattice constants, as well as B_0 and B_0' (for U=2.5 eV) are given in Table I. The LDA total-energy calculations yield equilibrium lattice parameters for the AmX, which are 5–8% smaller than their experimental counterparts. LDA$+U$ total energy calculations with U=2.5 eV, however, give values which are about 4–5% smaller than the experimental values. It is an established fact that the LDA usually underestimates the lattice parameter and overestimates the binding energy. However, the deviations obtained for the AmX are too large and point to a deficit in the LDA localization treatment of the Am-$5f$ electrons. SO coupling may counteract the LDA overbinding due to excess electronic pressure arising from the filled relativistic $f_{5/2}$ subband as was observed in calculations for the Pu monochalcogenides,[21] but this effect does not suffice to provide large enough lattice parameters. The LDA$+U$ approach clearly predicts lattice parameters closer to the experiment, which supports a substantial degree of $5f$ localization in the AmX. The Coulomb U of 4 eV yields somewhat better equilibrium volumes, as compared to the experiment, but it also yields a higher total energy as compared to U=2.5 eV (see Fig. 4). Thus, while we do not want to put emphasis on a particular U value, the more stable state would be attained for a U of about 2.5 eV. For this value, the bulk modulus decreases monotonously while its pressure derivative remains almost constant along the series (see Table I).

D. Magnetic susceptibility

Apart from the equilibrium lattice parameters, not many physical properties have been measured for the Am monop-

nictides. One of the few measured properties is the magnetic susceptibility χ. The Am monopnictides were reported[23–25] to exhibit a very high, temperature-independent susceptibility of $\sim 0.50-1.25\times10^{-3}$ emu/mol. In a previous attempt[31] to explain the high susceptibility, Pauli paramagnetism was assumed in conjunction with a high $5f$ density of states at E_F. In this explanation, the modified Pauli paramagnetic susceptibility is expressed by $\chi=\mu_B^2 N(E_F)$, with $N(E_F)$ being the density of states at E_F and μ_B the Bohr magneton. In the SIC-LSDA approach of Ref. 31, indeed, a very high $5f$ DOS is obtained at E_F, which could give rise to an extremely high Pauli susceptibility. The recent photoemission experiments, however, detect no $5f$-related emission near the Fermi energy.[1] Our LDA and LDA+U calculations also do not predict a high $5f$ DOS in the vicinity of E_F; the Pauli paramagnetic χ calculated from the very small DOS at E_F would be smaller than the experimental data by three orders of magnitude or even more.

Therefore, we suggest that the magnetic behavior of the Am pnictides can be explained by a Van Vleck susceptibility, which, for atoms, can appear for a $J=0$ ground state when a gap exists between the ground state and first-excited state. The Van Vleck atomic susceptibility is expressed by

$$\chi = 2N_A\mu_B^2 \sum_n \frac{|M_{0n}|^2}{E_n - E_0}, \tag{2}$$

where N_A is Avogadro's number, E_n-E_0 is the energy difference between the ground and first-excited states, and M_{0n} is the matrix element of $\mathbf{l}_z+2\mathbf{s}_z$ between the ground and excited states. Our aim is to approximate Eq. (2) to estimate values for the Van Vleck susceptibilities of the Am monopnictides. To this end, we need the appropriate equivalent of the energy difference in the formulation for periodic solids. A derivation of the Van Vleck susceptibility for energy band states in a periodic solid is given in the Appendix. The Van Vleck susceptibility (per unit cell) is calculated to be

$$\chi = 2\mu_B^2 \sum_{\substack{n\ un. \\ m\ occ.}} \sum_{\mathbf{k}} \frac{|\langle \mathbf{k}n|2s_z|\mathbf{k}m\rangle|^2}{E_{n\mathbf{k}} - E_{m\mathbf{k}}}, \tag{3}$$

where $|n\mathbf{k}\rangle$ are the Bloch band states and $E_{n\mathbf{k}}$ are the corresponding band energies. From Eq. (3), it can be recognized that the direct energy gap E_g between energy bands is the equivalent of the energy difference between the ground and first-excited states in the Van Vleck atomic susceptibility. Combining this with Eq. (2), we can use the direct gap E_g to approximate the Van Vleck molar susceptibility by $\chi \approx (8N_A\mu_B^2)/E_g$. Note, that in the case of a vanishing band gap, the susceptibility does not diverge but, taking the limit appropriately, the intraband contribution reduces to the Pauli susceptibility (see the Appendix).

In the case of AmN, the magnetic susceptibility calculated according to this expression would give $\chi \approx 1.3\times10^{-3}$ emu/mol, which compares reasonably to the experimental value of 0.78×10^{-3} emu/mol.[24] For the other Am monopnictides, the direct gaps in the LDA+U calculation would lead to Van Vleck susceptibilities of $0.95-1.15\times10^{-3}$ emu/mol. The direct gaps obtained within the LDA calculation are quite small ($\sim$150 meV) and would lead to higher Van Vleck susceptibilities ($\sim 1.7\times10^{-3}$ emu/mol) than those that were experimentally obtained. Nevertheless, the Van Vleck mechanism would predict the correct order of magnitude for the susceptibility.

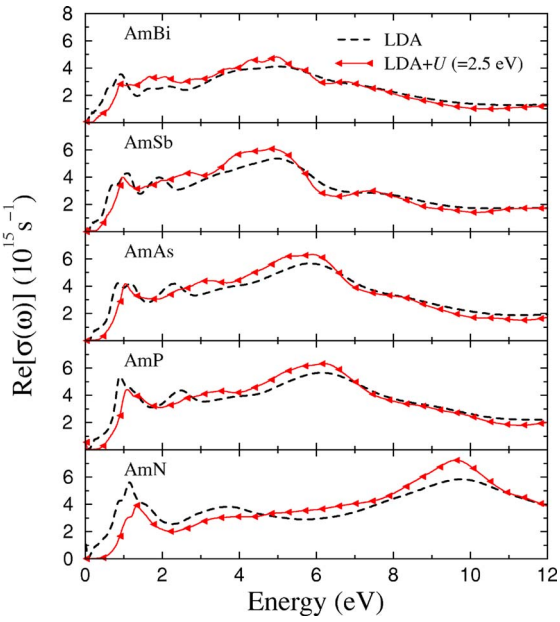

FIG. 5. (Color online) The absorptive part of the optical conductivity, Re$[\sigma(\omega)]$, as computed by the LDA and LDA+U approaches for the Am monopnictides.

E. Optical conductivity

Information about the energy positions of different electronic states can be derived from optical studies. The complex dielectric function $\varepsilon(\omega)$ is related to the optical conductivity $\sigma(\omega)$ by $\varepsilon(\omega)=1+4\pi i\sigma(\omega)/\omega$. The optical conductivity can be computed from the energy-band structure using the common linear-response expression (e.g., see Ref. 47)

$$\sigma(\omega) = \frac{e^2}{8m^2\pi^2\omega}\sum_{nn'}\int_{\mathrm{BZ}} d\mathbf{k}|P_{nn'}(\mathbf{k})|^2\delta(E_{n\mathbf{k}} - E_{n'\mathbf{k}} - \hbar\omega). \tag{4}$$

Here $P_{nn'}$ is the matrix element of the momentum operator, $P_{nn'}\equiv\langle n\mathbf{k}|p|n'\mathbf{k}\rangle$. For a cubic solid, one has $P\equiv P_x=P_y=P_z$. The absorptive part of the interband-optical conductivity, i.e., Re$[\sigma(\omega)]$, has been calculated from Eq. (4) using both the LDA and LDA+U approaches. The computed spectra are shown in Fig. 5. A notable difference exists between the LDA and LDA+U spectra in the low-energy region 0–4 eV, which is caused by the differences in the energy positions of the $5f$s. In the LDA+U, the low-energy absorption below 1 eV is reduced due to the removal of the $5f$ states which, consequently, do not take part in the interband transitions in this energy interval. Also, the direct optical

gaps become larger in the LDA+U spectra (note that the calculated spectra have been lifetime broadened through convolution with a Lorentzian with an inverse lifetime of 0.34 eV). The conductivity spectra show—for each of the monopnictides—three major peaks. For AmN these are located just above 1 eV, 3.5 eV, and ~9.5 eV. For the heavier pnictogen anions, these peaks shift successively to lower energies. For the bismuthide, these peaks are located slightly below 1 eV, at 2 eV, and ~5 eV. The origin of the peaks for AmN are as follows: the peak at 1 eV stems mainly from d-f transitions, which, in reciprocal space, occur along the Γ-X direction. The second peak at 3.5 eV arises from various interband transitions involving hybridized p, d, and f states, taking place along different BZ directions. The broad peak near 9.5 eV arises mainly from $p \rightarrow d$ transitions and some $f \rightarrow d$ transitions as well. Traversing the pnictogen series from N to Bi, the peaks shift to lower energies, because the unoccupied Am d and f bands move closer to E_F and the main weight of the occupied pnictogen p band moves closer to E_F as well. The partial DOS as depicted in Fig. 3 shows that the states around −2 eV are mainly of pnictogen p and Am d character. The third peak of AmN is observed at a high energy of 9.5 eV, because a substantial part of the nitrogen p band is located deeper below E_F than for the other pnictides. The later peak is located at energies between 4–6 eV for the other pnictides and it is primarily due to p-d transitions with some admixture of f-d transitions.

IV. DISCUSSIONS AND CONCLUSIONS

Previously not much was known about the electronic structure of the americium monopnictides. Our LDA as well as LDA+U calculations indicate that the Am monopnictides display either narrow-gap semiconducting behavior or pseudogap behavior. A third approach, which is often applied to compute f-electron materials, is the f-core method, in which the occupied f states are treated as unhybridized core electrons. In order to estimate the effect of complete 5f localization on the AmX electronic structures, we performed calculations with the f-core scheme as well. Also this approach to treat the 5f electrons led to pseudogap behavior for the Am monopnictides. On account of its small lattice parameter, the behavior of AmN deviates from that of the other monopnictides. The origin of the gap formation is the large SO interaction of Am which splits the Am-5$f_{5/2}$ and Am-5$f_{7/2}$ subbands away from E_F, in combination with the f-d and f-p hybridization. The inclusion of the Coulomb U leads to an additional shift of the 5$f_{5/2}$ and 5$f_{7/2}$ subbands away from E_F, with an extremely small DOS remaining at the Fermi level. The obtained semiconducting behavior and the very low density of states at E_F agree very well with the first photoemission studies performed on AmN and AmSb.[1] The photoemission studies show, indeed, a practically vanishing valence-band response in the vicinity of the Fermi edge and a broad, 5f response at binding energies of ~2–4 eV. As mentioned before, such binding energies correspond well with the positions of the f bands in the LDA+U calculations (see Fig. 3).[48] The LDA places the main occupied 5f band at binding energies of 1–2 eV, which are too small compared to the photoemission data. The presence of an excitation gap in the Am monopnictides is supported also by the measured high magnetic susceptibilities, which can be compellingly explained by a Van Vleck mechanism. On account of the computed 5f-occupation numbers being close to 6 for all monopnictides, Am is in a trivalent state ($5f^6, J=0$). AmN is the only monopnictide which shows a somewhat different behavior because of its small lattice parameter. Under pressure, the Am-5f occupation is reduced while the d occupation increases. This might lead to a mixed-valence state of trivalent and tetravalent Am ions.

Our calculations suggest electronic structures for the Am monopnictides which are in several respects different from the SIC-LSDA calculations of Ref. 31. The SIC-LSDA calculations also predict a trivalent Am configuration, but in addition it predicts the Am pnictides to be metallic with a very high 5f density of states at E_F. Such high DOS would actually render the Am pnictides to be heavy-fermion materials. While further experiments are undoubtedly needed to understand better the behavior of the Am-5f electrons, the photoemission experiments did not detect any f response near the Fermi edge.[1] Also, the valence-band signal vanished smoothly at the Fermi edge, suggesting the Am pnictides to be semiconductors.

The agreement between the experimental and LDA+U computed lattice parameters suggests a fair amount of localization of the Am-5f electrons. The strong SO interaction causes a split of the 5f subbands, removing them from the Fermi level and the Coulomb U adds a further splitting of the f subbands on top of that. We note, however, that the localization of the 5fs is still much less than that seen for the related lanthanide pnictides. This can be recognized from the evolution of the equilibrium lattice parameters across the lanthanide and actinide monopnictide series (for plots, see Refs. 20 and 21). While the lanthanide monopnictide series clearly shows the typical lanthanide lattice contraction with increasing atomic number, such behavior does not occur in the corresponding actinide series about Am. In this series, going from the Pu monopnictide to its Am equivalent and to the curium equivalent there is an *increase* in the lattice constant. This increase is the largest for the lighter pnictogen atoms and levels off for the heavier pnictogens (the lattice parameter of CmBi is not precisely known). The localization tendency, thus, appears to be the largest for the heavier pnictogen anions, Sb and Bi.

Among the lanthanide compounds[2–5] and actinide compounds[10–12] as well, there are several narrow-gap materials. Some of these have been classified as Kondo insulators, in which a correlated magnetic coupling of valence electrons to the localized f electrons leads to gap formation. The mechanism leading to gap formation in the Am monopnictides is distinctly different. The precursor to the gap formation is the large SO interaction, which removes the 5fs from the vicinity of E_F. If we artificially reduce the Am SO interaction in the calculations, we immediately obtain the Am monopnictides to be metals. Furthermore, there are the f-d and f-p hybridizations, which contribute to the gap formation, in a way similar as demonstrated previously for the Pu

monochalcogenides.[21] Thus, the actinide rocksalt compounds differ from the corresponding rare earths for two reasons: (i) relativistic effects lead to prominent changes in the energy positions of the actinide f states and (ii) the larger spatial extension of the $5f$ wave functions results in an increased hybridization with other states.

To further elucidate the electronic structure of the Am monopnictides, we suggest resistivity and infrared reflectivity measurements to probe their conducting properties. Measurements of the resistivity and lattice parameter under pressure are also desirable as these could show changes of the gap and, particularly for AmN, changes of the $5f$ valency.

ACKNOWLEDGMENTS

We gratefully thank T. Gouder, F. Wastin, G. H. Lander, and O. Eriksson for valuable discussions. This work is funded under the exchange programme between the Department of Science and Technology (DST), Grant No. INT/DST/DAAD/P-49/2001, the government of India, and the German DAAD Grant No. 0026524, and by the German Sonderforschungsbereich 463, Dresden.

APPENDIX: DERIVATION OF VAN VLECK SUSCEPTIBILITY

The interaction Hamiltonian for an applied field $\mathbf{H}$ is

$$\mathcal{H}' = -\mu_B \mathbf{H}\cdot\mathbf{m} \tag{A.1}$$

in μ_B with $\mathbf{m}=\mathbf{l}+2\mathbf{s}$. In terms of the Green's function, the electron number and magnetic moment are

$$n = \mathrm{Tr}\,\rho = \frac{1}{2\pi i}\oint_{E_F} dz\,\mathrm{Tr}\,G(z),$$

$$\mathbf{m} = \mathrm{Tr}\{\mathbf{m}\rho\} = \frac{1}{2\pi i}\oint_{E_F} dz\,\mathrm{Tr}\{\mathbf{m}G(z)\}, \tag{A.2}$$

where G contains 2×2 spin-matrix components.

The Dyson equation for the Green's function is

$$G = G^0 + G^0\mathcal{H}'G = G^0 + G^0\mathcal{H}'G^0 + \cdots, \tag{A.3}$$

where, for linear response, only the first two terms in the expansion are required. The change in the Fermi energy, due to the applied field, is second order in the field. The induced moment is, therefore, to first order in a magnetic field H_z applied along the z direction,

$$m_z = \frac{-H_z}{2\pi i}\oint_{E_F} dz\,\mathrm{Tr}\{m_z G^0(z) m_z G^0(z)\} \tag{A.4}$$

and the uniform magnetic susceptibility is consequently

$$\chi = \frac{-1}{2\pi i}\oint_{E_F} dz\,\mathrm{Tr}\{m_z G^0(z) m_z G^0(z)\}. \tag{A.5}$$

For pure spin magnetism, we have $m_z=2s_z\mu_B=\sigma_z\mu_B$ and, since σ_z commutes with G^0 and $\sigma_z^2=1$, the susceptibility becomes

$$\chi = \frac{-\mu_B^2}{2\pi i}\mathrm{Tr}\oint_{E_F} dz G^0(z)^2 = \frac{\mu_B^2}{2\pi i}\mathrm{Tr}\oint_{E_F} dz\frac{dG^0(z)}{dz}$$
$$= -\frac{\mu_B^2}{\pi}\,\mathrm{Im\,Tr}\,G^0(E_F) = \mu_B^2 N(E_F), \tag{A.6}$$

where $N(E_F)$ is the density of states at the Fermi level. Thus, we obtain Pauli paramagnetism.

In the presence of the spin-orbit interaction, the Green's function commutes with neither σ_z nor m_z since it has off-diagonal components in spin. If the solutions to the wave equation in the presence of spin-orbit interaction are denoted by $|\mathbf{k}n\rangle$, we can rewrite the trace in Eq. (A.5) using that $G^0(z)=(z-\mathcal{H}^0)^{-1}$

$$\mathrm{Tr}\{m_z G^0(z) m_z G^0(z)\} = \sum_{nm,\mathbf{k}} \langle \mathbf{k}n|m_z G^0|\mathbf{k}m\rangle\langle \mathbf{k}m|m_z G^0|\mathbf{k}n\rangle$$
$$= \sum_{nm,\mathbf{k}} |\langle \mathbf{k}n|m_z|\mathbf{k}m\rangle|^2 \frac{1}{z-E_{m\mathbf{k}}}\frac{1}{z-E_{n\mathbf{k}}}. \tag{A.7}$$

The contour integral Eq. (A.5) has to enclose the poles on the energy axis up to the chemical potential. The integration can be chosen along $z=E^+=E+i\epsilon$ and $z=E^-=E-i\epsilon$, which, together with $1/E^+=\mathcal{P}(1/E)-\pi i\delta(E)$ gives

$$\chi = \frac{-1}{2\pi i}\int_{-\infty}^{E_F} dE \sum_{nm,\mathbf{k}} |M^z_{nm}|^2 \frac{1}{E^- - E_{m\mathbf{k}}}\frac{1}{E^- - E_{n\mathbf{k}}}$$
$$- \frac{1}{2\pi i}\int_{E_F}^{-\infty} dE \sum_{nm,\mathbf{k}} |M^z_{nm}|^2 \frac{1}{E^+ - E_{m\mathbf{k}}}\frac{1}{E^+ - E_{n\mathbf{k}}}$$
$$= \frac{-1}{2\pi i}\int_{-\infty}^{E_F} dE \sum_{nm,\mathbf{k}} |M^z_{nm}|^2 \left[\mathcal{P}\frac{1}{E-E_{m\mathbf{k}}} + \pi i\delta(E-E_{m\mathbf{k}})\right]$$
$$\times\left[\mathcal{P}\frac{1}{E-E_{n\mathbf{k}}} + \pi i\delta(E-E_{n\mathbf{k}})\right]$$
$$+ \frac{1}{2\pi i}\int_{-\infty}^{E_F} dE \sum_{nm,\mathbf{k}} |M^z_{nm}|^2 \left[\mathcal{P}\frac{1}{E-E_{m\mathbf{k}}} - \pi i\delta(E-E_{m\mathbf{k}})\right]$$
$$\times\left[\mathcal{P}\frac{1}{E-E_{n\mathbf{k}}} - \pi i\delta(E-E_{n\mathbf{k}})\right], \tag{A.8}$$

where M^z_{nm} is introduced for the spin-matrix element. After a straightforward integration, the susceptibility becomes

$$\chi = -\mathcal{P}\sum_{nm,\mathbf{k}} |\langle \mathbf{k}n|m_z|\mathbf{k}m\rangle|^2 \frac{f(E_{n\mathbf{k}}) - f(E_{m\mathbf{k}})}{E_{n\mathbf{k}} - E_{m\mathbf{k}}}. \quad \text{(A.9)}$$

The interband matrix elements are the equivalent of the Van Vleck contribution for localized systems. The intraband contribution reduces again [with $\partial f/\partial E \rightarrow -\delta(E-E_F)$] to the equivalent of the Pauli susceptibility. In the interband case, the double sum can be further rewritten by separating the occupied and unoccupied states, which, for the spin susceptibility at $T \approx 0$, gives

$$\chi = 8\mu_B^2 \sum_{\substack{n\,un. \\ m\,occ.}} \sum_{\mathbf{k}} \frac{|\langle \mathbf{k}n|s_z|\mathbf{k}m\rangle|^2}{E_{n\mathbf{k}} - E_{m\mathbf{k}}}. \quad \text{(A.10)}$$

This has to be multiplied by Avogadro's number to obtain the molar susceptibility. The interband matrix elements are diagonal in the wave vector; therefore, the direct band gap is to be used to evaluate the Van Vleck susceptibility.

*Present address: Dept. of Physics, Uppsala University, Box 530, S-751 21 Uppsala, Sweden.

[1] T. Gouder, P. M. Oppeneer, F. Huber, F. Wastin, and J. Rebizant, preceding paper, Phys. Rev. B **72**, 115122 (2005).

[2] P. S. Riseborough, Adv. Phys. **49**, 257 (2000).

[3] P. Wachter, in *Handbook on the Physics and Chemistry of the Rare Earths*, edited by K. A. Gschneidner, Jr., L. Eyring, G. H. Lander, and G. R. Choppin (Elsevier, Amsterdam, 1994), Vol. 19, p. 177.

[4] L. Degiorgi, Rev. Mod. Phys. **71**, 687 (1999).

[5] G. Aeppli and Z. Fisk, Comments Condens. Matter Phys. **16**, 155 (1992).

[6] A. J. Arko, P. S. Riseborough, A. B. Andrews, J. J. Joyce, A. N. Tahvildar-Zadeh, and M. Jarrel, in *Handbook on Physics and Chemistry of the Rare Earths*, edited by K. A. Gschneidner, Jr. and L. Eyring (Elsevier, Amsterdam, 1999) Vol. 26, p. 265.

[7] P. M. Oppeneer, A. Y. Perlov, V. N. Antonov, A. N. Yaresko, T. Kraft, and M. S. S. Brooks, J. Alloys Compd. **271–273**, 831 (1998).

[8] A. J. Arko, J. J. Joyce, L. Morales, J. Wills, J. Lashley, F. Wastin, and J. Rebizant, Phys. Rev. B **62**, 1773 (2000).

[9] E. Guziewicz, T. Durakiewicz, M. T. Butterfield, C. G. Olson, J. J. Joyce, A. J. Arko, J. L. Sarrao, D. P. Moore, and L. Morales, Phys. Rev. B **69**, 045102 (2004).

[10] V. Ichas, J. C. Griveau, J. Rebizant, and J. C. Spirlet, Phys. Rev. B **63**, 045109 (2001).

[11] P. de V. du Plessis, A. M. Strydom, R. Troć, and L. Menon, J. Phys.: Condens. Matter **13**, 8375 (2001).

[12] R. Troć, A. M. Strydom, P. de V. du Plessis, V. H. Tran, A. Czopnik, and J. K. Cockroft, Philos. Mag. **83**, 1235 (2003).

[13] A. J. Freeman and D. D. Koelling, in *The Actinides: Electronic Structure and Related Properties*, edited by A. J. Freeman and J. B. Darby, Jr. (Academic Press, New York, 1974), Vol. 1, p. 51.

[14] S. S. Hecker and L. F. Timofeeva, Los Alamos Sci. **26**, 244 (2000).

[15] J. R. Naegele, L. Manes, J. C. Spirlet, and W. Müller, Phys. Rev. Lett. **52**, 1834 (1984).

[16] S. Heathman, R. G. Haire, T. Le Bihan, A. Lindbaum, K. Litfin, Y. Méresse, and H. Libotte, Phys. Rev. Lett. **85**, 2961 (2000).

[17] T. Gouder, F. Wastin, J. Rebizant, and L. Havela, Phys. Rev. Lett. **84**, 3378 (2000).

[18] J. J. Joyce, J. M. Wills, T. Durakiewicz, M. T. Butterfield, E. Guziewicz, J. L. Sarrao, L. A. Morales, A. J. Arko, and O. Eriksson, Phys. Rev. Lett. **91**, 176401 (2003).

[19] T. Durakiewicz, J. J. Joyce, G. H. Lander, C. G. Olson, M. T. Butterfield, E. Guziewicz, A. J. Arko, L. Morales, J. Rebizant, K. Mattenberger, and O. Vogt, Phys. Rev. B **70**, 205103 (2004).

[20] J. P. Charvillat, U. Benedict, D. Damien, C. H. de Novion, A. Wojakowski, and W. Müller, in *Transplutonium 1975*, edited by W. Müller and R. Lindner (North-Holland, Amsterdam, 1976), p. 79.

[21] P. M. Oppeneer, T. Kraft, and M. S. S. Brooks, Phys. Rev. B **61**, 12825 (2000).

[22] P. Burlet, S. Quezel, J. Rossat-Mignod, J. C. Spirlet, J. Rebizant, W. Müller, and O. Vogt, Phys. Rev. B **30**, 6660 (1984).

[23] B. D. Dunlap, D. J. Lam, G. M. Kalvius, and G. K. Shenoy, J. Appl. Phys. **42**, 1719 (1971).

[24] B. Kanellakopulos, J. P. Charvillat, F. Maino, and W. Müller, in *Transplutonium 1975*, edited by W. Müller and R. Lindner (North-Holland, Amsterdam, 1976), p. 181.

[25] O. Vogt, K. Mattenberger, J. Löhle, and J. Rebizant, J. Alloys Compd. **271–273**, 508 (1998).

[26] J. M. Fournier, E. Pleska, J. Chiapusio, J. Rossat-Mignod, J. C. Spirlet, and O. Vogt, Physica B **163**, 493 (1990).

[27] P. Wachter, F. Marabelli, and B. Bucher, Phys. Rev. B **43**, 11136 (1991); P. Wachter, Solid State Commun. **127**, 599 (2003).

[28] M. D. Jones, J. C. Boettger, R. C. Albers, and D. J. Singh, Phys. Rev. B **61**, 4644 (2000).

[29] M. S. S. Brooks, J. Phys. F: Met. Phys. **14**, 639 (1984).

[30] T. Kraft, P. M. Oppeneer, V. N. Antonov, and H. Eschrig, Phys. Rev. B **52**, 3561 (1995).

[31] L. Petit, A. Svane, W. M. Temmerman, and Z. Szotek, Phys. Rev. B **63**, 165107 (2001).

[32] P. M. Oppeneer, A. N. Yaresko, A. Y. Perlov, V. N. Antonov, and H. Eschrig, Phys. Rev. B **54**, R3706 (1996); A. B. Shick and W. E. Pickett, Phys. Rev. Lett. **86**, 300 (2001); H. Harima, J. Magn. Magn. Mater. **226–230**, 83 (2001); A. N. Yaresko, V. N. Antonov, and P. Fulde, Phys. Rev. B **67**, 155103 (2003).

[33] S. Y. Savrasov and G. Kotliar, Phys. Rev. Lett. **84**, 3670 (2000).

[34] J. Bouchet, B. Siberchicot, F. Jolleti, and A. Pasturel, J. Phys.: Condens. Matter **12**, 1723 (2000).

[35] A. B. Shick, V. Drchal, and L. Havela, Europhys. Lett. **69**, 588 (2005); A. B. Shick, V. Janiš, and P. M. Oppeneer, Phys. Rev. Lett. **94**, 016401 (2005).

[36] A. W. Mitchell and D. J. Lam, J. Nucl. Mater. **37**, 349 (1970); J. W. Roddy, J. Inorg. Nucl. Chem. **36**, 2531 (1974).

[37] O. K. Andersen, Phys. Rev. B **12**, 3060 (1975).

[38] S. Y. Savrasov and D. Y. Savrasov, Phys. Rev. B **46**, 12181 (1992); S. Y. Savrasov, Phys. Rev. B **54**, 16470 (1996).

[39] V. I. Anisimov, I. V. Solovyev, M. A. Korotin, M. T. Czyzyk, and

G. A. Sawatzky, Phys. Rev. B **48**, 16929 (1993); A. I. Liechtenstein, V. I. Anisimov, and J. Zaanen, Phys. Rev. B **52**, R5467 (1995).

[40] D. B. Ghosh, M. De, and S. K. De, Phys. Rev. B **67**, 035118 (2003).

[41] H. Ogasawara, A. Kotani, and B. T. Thole, Phys. Rev. B **44**, 2169 (1991).

[42] The choice of the spin s_z and m_l angular momentum quantum numbers has been made such that the spin and orbital polarization remains zero and that all six j_z states of the $j_{5/2}$ manifold are included. These constraints enforce three spin-up and three spin-down states, where the spin-up and spin-down states are to be combined each with opposite m_l quantum numbers. This leaves us with three possible sets of s_z, m_l combinations. As effectively, the same six j_z states are affected by the Coulomb U, the results will almost coincide.

[43] In the heavier actinides, spin-orbit coupling and exchange interaction counteract each other in the formation of a magnetic or nonmagnetic ground state. The emerging ground state may depend sensitively on the chosen parameter values in the LDA $+U$ calculation (see Ref. 35).

[44] M. S. S. Brooks, J. Magn. Magn. Mater. **63&64**, 649 (1987).

[45] J. P. Perdew and M. Levy, Phys. Rev. Lett. **51**, 1884 (1983); L. J. Sham and M. Schlüter, Phys. Rev. Lett. **51**, 1888 (1983).

[46] J. F. Herbst, R. E. Watson, and I. Lindgren, Phys. Rev. B **14**, 3265 (1976); M. S. S. Brooks, B. Johansson, O. Eriksson, and H. L. Skriver, Physica B & C **144B**, 1 (1986).

[47] J. Callaway, *Quantum Theory of Solids* (Academic Press, New York, 1974).

[48] The SIC-LSDA approach (Ref. 32) places the occupied f states much deeper below E_F at energies of ~ -10 to -20 eV.